



## Formation of essential oil containing microparticles comprising a hydrogenated vegetable oil matrix and characterisation thereof

Pia Gottschalk, Benjamin Brodesser, Denis Poncelet, Henry Jaeger, Harald Rennhofer & Stephen Cole

To cite this article: Pia Gottschalk, Benjamin Brodesser, Denis Poncelet, Henry Jaeger, Harald Rennhofer & Stephen Cole (2018): Formation of essential oil containing microparticles comprising a hydrogenated vegetable oil matrix and characterisation thereof, Journal of Microencapsulation, DOI: [10.1080/02652048.2018.1515998](https://doi.org/10.1080/02652048.2018.1515998)

To link to this article: <https://doi.org/10.1080/02652048.2018.1515998>



Accepted author version posted online: 30 Aug 2018.  
Published online: 27 Dec 2018.



Submit your article to this journal [↗](#)



Article views: 17



View Crossmark data [↗](#)



# Formation of essential oil containing microparticles comprising a hydrogenated vegetable oil matrix and characterisation thereof

Pia Gottschalk<sup>a,b,c</sup>, Benjamin Brodesser<sup>c</sup>, Denis Poncelet<sup>a</sup>, Henry Jaeger<sup>b</sup>, Harald Rennerhofer<sup>b</sup> and Stephen Cole<sup>c</sup> 

<sup>a</sup>Oniris, UMR CNRS 6144 GEPEA, Nantes, France; <sup>b</sup>University of Natural Resources and Life Sciences, Vienna, Austria; <sup>c</sup>Biomin Research Centre, Technopark 1, Tulln, Austria

## ABSTRACT

Microparticles with different essential oil concentrations 0, 75, 150, 225 and 300 g kg<sup>-1</sup>, (g of essential oil per kg of microparticles), were produced by dispersing the essential oils within a hydrogenated vegetable fat matrix and forming spherical solid particles by spray-chilling. Size distribution, flowability, surface structure, essential oil recovery, melting properties and crystallinity of the microparticles were determined. With over 225 g kg<sup>-1</sup> essential oil the microparticle surface became stickier, their flowability was reduced and the size distribution broadened. Gas chromatography showed that the essential oil recovery was always above 85% v/v. The surface structure of the microparticles was strongly affected by the essential oil concentration being smooth (225 g kg<sup>-1</sup>), comprising round-shaped bumps (300 g kg<sup>-1</sup>) or showing fat blooming (0, 75, 150 g kg<sup>-1</sup>). With essential oil, the formation of the  $\beta$ -polymorphic form of the triglycerides was supported leading to changes in the melting behaviour and the crystalline structure.

## ARTICLE HISTORY

Received 22 May 2018  
Accepted 21 August 2018

## KEYWORDS

Essential oils; microencapsulation; spray-chilling; hydrogenated vegetable fat; melting behaviour; crystallinity

## 1. Introduction

Essential oils are mixtures of volatile compounds produced by plants. Due to their antibacterial, antifungal and antiviral activities, essential oils are nowadays widely used in the food and feed industry (El Asbahani *et al.* 2015). Furthermore, their positive effect on growth performance, gut microbiota and the welfare of monogastric animals make essential oils interesting as replacers for antibiotic growth promoters (Bento *et al.* 2013, Murugesan *et al.* 2015, Zeng *et al.* 2015, Suresh *et al.* 2018). However, their volatile character renders the application of essential oils in food and feed and especially in dry feed mixtures rather difficult. In general, microencapsulation is a technique to increase the storage stability of essential oils, mask their flavour, protect them from interactions with other nutrients, reduce the risk of oxidation and enable their controlled release (Vishwakarma *et al.* 2016). Hydrophobic coating or matrix materials are widely used in the animal feed industry to protect active ingredients such as essential oils from digestive activities in the rumen or to control their release throughout the gastro-intestinal tract of the target animal (Klose 2000, Popplewell and Porzio 2001, Gately *et al.* 2009).

Encapsulation defines the process of entrapping an active material, the so-called core material, into another material (shell or matrix), such as lipids, gums, proteins, polysaccharides or polymers. Depending on the selected encapsulation process, the active material is either surrounded by a coating (core shell encapsulation) or finely dispersed within a matrix (matrix encapsulation) (Gibbs *et al.* 1999, Bakry *et al.* 2016). Microencapsulation of essential oils can be realised via spray cooling/chilling. Herein, the active material is mixed with a molten carrier material, such as a hydrogenated vegetable oil or a wax. The mixture is subsequently atomised and brought in contact with cool air forming microparticles by solidification. Spray chilling can either be realised with a spinning disc which makes use of centrifugal forces for droplet formation or with a spray nozzle. In both cases, almost perfectly spherical microparticles with a narrow size distribution can be produced. Sphericity can be a great advantage when the microparticles shall be furnished with an additional coating. Other advantages of the spray chilling technology and the use of hydrophobic matrix materials are the mild processing conditions, satisfying retention levels of volatile substances

and the comparatively uncomplicated up-scaling (Alvim *et al.* 2013).

The application of hydrophobic compounds as matrix or coating material in encapsulation processes requires the consideration of their physical properties. Fats and waxes can take on diverse polymorphic forms with the  $\alpha$ -form being the least stable but preferably occurring form due to its hexagonal crystal packing and the  $\beta$ -form being the most stable one with an orthorhombic-perpendicular crystalline structure (Mayama 2009, Lopes *et al.* 2015). Additionally, intermediate  $\beta'$ -forms can occur (Himawan *et al.* 2006, Sato 2001) characterised by a triclinic-parallel crystal lattice. The polymorphic transformation from the  $\alpha$ - over the  $\beta'$ - to the  $\beta$ -form can be influenced by the presence of additives such as surfactants and essential oils. Fats or waxes can also be exposed to desirable (e.g. a controlled heat treatment in an oven) or undesirable (e.g. storage at higher than optimal temperature) tempering processes which can enhance the polymorphic transformation (Lopes *et al.* 2015, Miyasaki *et al.* 2016).

The aim of this study was to investigate the impact of the process and the essential oil concentration on the physico-chemical properties of spray-chilled microparticles using hydrogenated vegetable fat as matrix material. The essential oil containing microparticles used in this study are destined to be utilised in an animal feed additive. The matrix encapsulation of the essential oils enables the additive to be protected through compound animal feed manufacture and to subsequently control the release of the active essential oils in the gastro-intestinal tract of the animal following feeding. The protective and delayed-release characteristics of such microparticles are relevant for other applications, particularly in the food (Jackson and Lee 1991, Madene *et al.* 2006) and pharmaceutical industries (Singh *et al.* 2010).

## 2. Materials and methods

### 2.1. Chemicals

Hydrogenated vegetable oil (VGB 5ST, melting point 69–73 °C, CAS: 91082–37-0) was purchased from ADM Sio (Fourqueux, France). Hydrophobic, precipitated silicate (Sipernat D17,  $D_{50}$  10  $\mu\text{m}$ , specific surface area 100  $\text{m}^2/\text{g}$ , CAS: 68611–44-9) was purchased from Evonik (Essen, Germany). The essential oil mixture used as the active ingredient was a proprietary blend (major component (70% v/v) carvacrol together with thymol, carvone and linalool) from Biomin<sup>®</sup> Phytogenics GmbH (Stadtoldendorf, Germany).

### 2.2. Preparation of the microparticles

Hydrogenated vegetable oil was heated on a digital magnetic stirrer (IKA Model RCTB, IKA-Werke GmbH & Co, Staufen, Germany) to 85 °C until molten and different amounts of the essential oil mixture were added with continuous mixing (300 rpm). The molten mixtures were atomised by spinning disc (6 cm diameter, 2000–3000 rpm, Sprai SAS, Orsay, France) and solidified by cooling at room temperature in a self-constructed process chamber (approx. 2 × 2 × 2 m). Microparticles were collected at a controlled distance, indicated by the spinning disc controlling software, from the centre of the atomiser.

### 2.3. Microparticle characterisation

#### 2.3.1. Particle size analysis

Particle size analysis was performed by laser diffraction using a Beckman LS 13320 (Beckman-Coulter GmbH, Vienna, Austria) with a universal liquid module and propan-2-ol (Carl Roth, Germany) as dispersant. The measurement duration was set to 15 s. A pump speed of 40% and an obscuration of 15% were selected.

The dispersion (span) was calculated from the volumetric mean ( $D_{50}$ ) of the microparticles with the following formula:

$$\text{Span} = \frac{D_{90} - D_{10}}{D_{50}} \quad (1)$$

where  $D_{90}$  = diameter corresponding to 90% of the volumetric cumulative particles fraction,

$D_{10}$  = diameter corresponding to 10% of the volumetric cumulative particles fraction and

$D_{50}$  = diameter corresponding to 50% of the volumetric cumulative particles fraction.

#### 2.3.2. Encapsulation efficiency

The essential oil concentration in the microparticles, from which the encapsulation efficiency can be calculated, was determined with a Shimadzu GC 2010 (Shimadzu, Austria) gas chromatograph with a FID detector and an Optima WAX plus (Machery-Nagel, Germany) column, 30 m length, 0.25 mm id. Essential oil was extracted by intensive mixing of 0.1 to 0.11 grams of microparticles with 1.5 ml ethyl acetate (Chem Labs, Bartelt, Graz, Austria), centrifugation (4000 rpm) and collection of the supernatant. The extraction was repeated three times. The instrument was operated with helium as carrier gas (1.2 ml/min). The oven programme started at 60 °C for 1 min, 5 °C/min to 85 °C, 25 °C/min to 150 °C, 6 °C/min to

200 °C, 30 °C/min to 270 °C hold 7 min. The FID detector was operated at 280 °C with a flow of hydrogen of 40 ml/min, air 400 ml/min, and helium as makeup gas 30 ml/min. The data rate was 25 Hz.

Knowing the essential oil concentration in the microparticles and the theoretically expected essential oil concentration, the encapsulation efficiency could be calculated using the following formula.

$$\text{Encapsulation efficiency [\%]} = \frac{\text{Essential oil concentration in the particles } \left[ \frac{\text{mg}}{\text{g}} \right]}{\text{Theoretically essential oil concentration } \left[ \frac{\text{mg}}{\text{g}} \right]} * 100 \quad (2)$$

### 2.3.3. Powder flowability

Powder flow was determined by angle of repose measurement. Microparticles were poured through a glass funnel onto a disc ( $r = 3$  cm) positioned 15 cm below. Angle of repose was obtained using the equation, where  $h$  is the height (cm) of the powder cone:

$$\tan \alpha = \frac{h}{r} \quad (3)$$

Empirical powder flowability was determined from the angle of repose (Lumay *et al.* 2012). Every determination was performed in triplicate.

### 2.3.4. Structural and morphological analysis

The surface of particles was investigated by light microscopy and scanning electron microscopy. Light microscopy was performed with a Leica M80 (Leica, Vienna, Austria,) stereomicroscope. Scanning electron microscopy analysis was either done with a Zeiss Supra 35 (Carl Zeiss Microscopy GmbH, Jena, Germany) or with a Quanta FEG 250 (FEI, Oregon). The images were recorded with the SE detector with a beam voltage of 3 or 5 kV, a beam current of 80  $\mu$ A and a spot size of 1–2 nm. The working distance was 5 mm. Samples investigated by scanning electron microscopy were either sputtered with carbon in a rotor Emitech K950x (Emitech, Maine, U.S.A) vacuum coater or with gold in a HHV Scancoat Six (HHV, Bangalore, India) compact sputter coater.

### 2.3.5. Investigation of the melting behaviour

The melting behaviour of microparticles was investigated by differential scanning calorimetry (DSC). Analysis was performed with a STA 449 F1 calorimeter (Netzsch, Selb, Germany) and the data evaluation with the Netzsch Proteus Thermal Analysis software Version

5.2.1. All measurements were performed in closed aluminium crucibles. Melting curves were determined at a standard heating rate of 10 K/min, which allows the clear expression of the melting peaks, between  $-50$  and  $90$  °C. Helium with a flow rate of 40 ml/min was used as the purging media. Calibration of the equipment was performed with adamantane, zinc, tin, bismuth and indium. Each measurement consisted of two melting cycles. The sample weight for all measurements was  $10 \pm 0.6$  mg.

### 2.3.6. Investigation of the crystalline structure

X-ray powder diffraction scattering was performed with a Rigaku SMax3000 (Rigaku, Tokyo, Japan) with a Triton200 (Rigaku, Tokyo, Japan) multiple wire detector for the small angle X-ray scattering and a Fuji Image Plate (Fuji, Tokyo, Japan) for wide angle X-ray diffraction. The wide angle X-ray scattering images were recorded in one single shot of 1800 s exposure time in the range of 1 to  $4.5 \text{ \AA}^{-1}$  (corresponding to 14 to 67 degree scattering angle) and the Fuji Image Plate was read out with a resolution of 0.0453 degrees scattering angle. The small angle X-ray scattering images were also recorded in one single shot but for 3600 s each in the range of 0.01 to  $1 \text{ \AA}^{-1}$ . A MM002+ micro focus X-ray tube with copper target (Cu-K $\alpha$ , wavelength 0.154 nm) and integrated confocal max-flux small angle X-ray scattering optics (Rigaku, Tokyo, Japan) was operated with 45 kV and 0.88 mA. The system uses a three-pinhole collimation to obtain a circular beam of about 210  $\mu$ m diameter on the sample. For the sample preparation, a small amount of the microparticles was fixed between two plastic stripes. The signal from the plastic stripes alone was subtracted from the signals coming from the samples to eliminate the background signal.

## 3. Results and discussion

### 3.1. Production of the particles

Several microparticle batches with essential oil concentrations ranging from 0 to 300 g kg $^{-1}$  were produced by spray-chilling applying the method described above. The crystallinity and the melting profile of the microparticles with 0 g kg $^{-1}$  essential oil were compared with the same parameters of the unprocessed hydrogenated fat-flakes to investigate the impact of the spray-chilling process. The impact of the presence and the concentration of essential oil was investigated by comparing the microparticles with varying essential oil concentration.

**Table 1.** Particle size distribution ( $n = 3$ ) of microparticles with differing essential oil concentration.

	Essential oil concentration ( $\text{gkg}^{-1}$ )				
	0	75	150	225	300
$D_{10}$ [ $\mu\text{m}$ ]	$121 \pm 5.1$	$117 \pm 5.9$	$145 \pm 0.6$	$135 \pm 1.1$	$148 \pm 1.1$
$D_{50}$ [ $\mu\text{m}$ ]	$182 \pm 5.1$	$175 \pm 6.4$	$201 \pm 1.6$	$199 \pm 1.7$	$237 \pm 4.7$
$D_{90}$ [ $\mu\text{m}$ ]	$250 \pm 5.1$	$241 \pm 7.6$	$271 \pm 2.4$	$289 \pm 7.5$	$488 \pm 42.2$
Span	0.71	0.71	0.63	0.77	1.44

The measured parameters exhibit a narrow size distribution for microparticles with up to  $225 \text{ gkg}^{-1}$  essential oil.

Sampling was performed within a certain radius from the centre of the spinning disc so that in theory the various microparticle batches should have had similar size distributions with a  $D_{50}$  value around  $200 \mu\text{m}$ .

### 3.2. Particle size

The particle size distribution of the different microparticles are shown in Table 1.

The microparticles without essential oil or with an essential oil concentration up to  $225 \text{ gkg}^{-1}$  exhibited a narrow size distribution. The size distribution of the microparticles with  $300 \text{ gkg}^{-1}$  essential oil was broader than for any other microparticle batch and the  $D_{90}$  value was increased by over  $100 \mu\text{m}$ , although those microparticles were collected in the same area as all the other batches. These observations might be explained with the microparticles surface getting stickier with increasing essential oil concentration and tending to attach to each other so that they are not detected as single particles but as agglomerates by the laser diffraction device. This assumption is supported by the fact that sampling after production got more and more difficult with increasing essential oil concentration as the microparticles tended to stick to the bottom of the spray-chilling tower. When these microparticles shall be added to a dry feed mixture accurate dosing might be problematic as the single particles cannot be separated without additional mechanical impact.

### 3.3. Encapsulation efficiency

The recovery of four of the individual compounds of the essential oil, linalool, carvone, thymol and carvacrol as a function of the essential oil concentration is presented in Figure 1. For all compounds, independently from the initial essential oil concentration, the recovery was higher than 85%. The recovery of linalool (the compound with the highest vapour pressure) was the lowest for all four initial essential oil concentrations. Additionally, the recovery of all four compounds

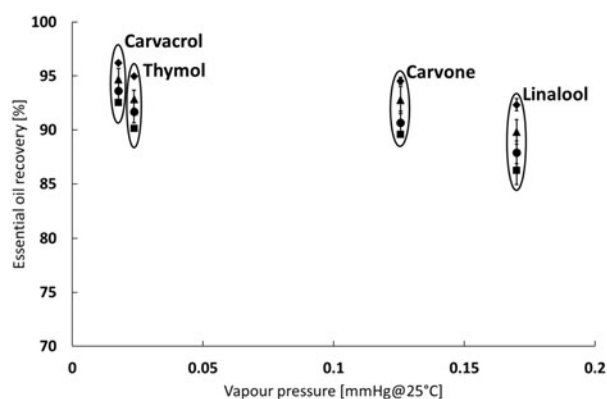


**Figure 1.** Recovery of the different essential oil compounds in the microparticles with  $75 \text{ gkg}^{-1}$  (■),  $150 \text{ gkg}^{-1}$  (●),  $225 \text{ gkg}^{-1}$  (▲) and  $300 \text{ gkg}^{-1}$  (◆) essential oil as a function of vapour pressure.

increased with increasing initial essential oil concentrations. For linalool, this increase was the biggest with approx. 7% difference compared to the microparticles with  $75 \text{ gkg}^{-1}$  essential oil. As the particle size distribution of the microparticles with  $300 \text{ gkg}^{-1}$  essential oil was broader and the  $D_{90}$  was  $100 \mu\text{m}$  bigger compared to all other batches, it could have been assumed that an increased amount of essential oil on the microparticle surface also leads to an increased loss.

### 3.4. Flowability

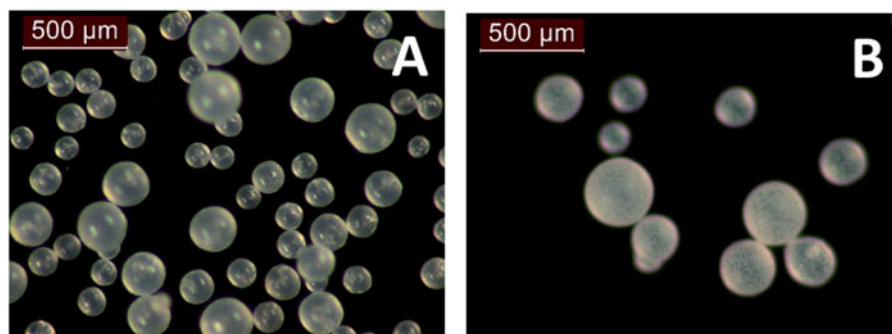
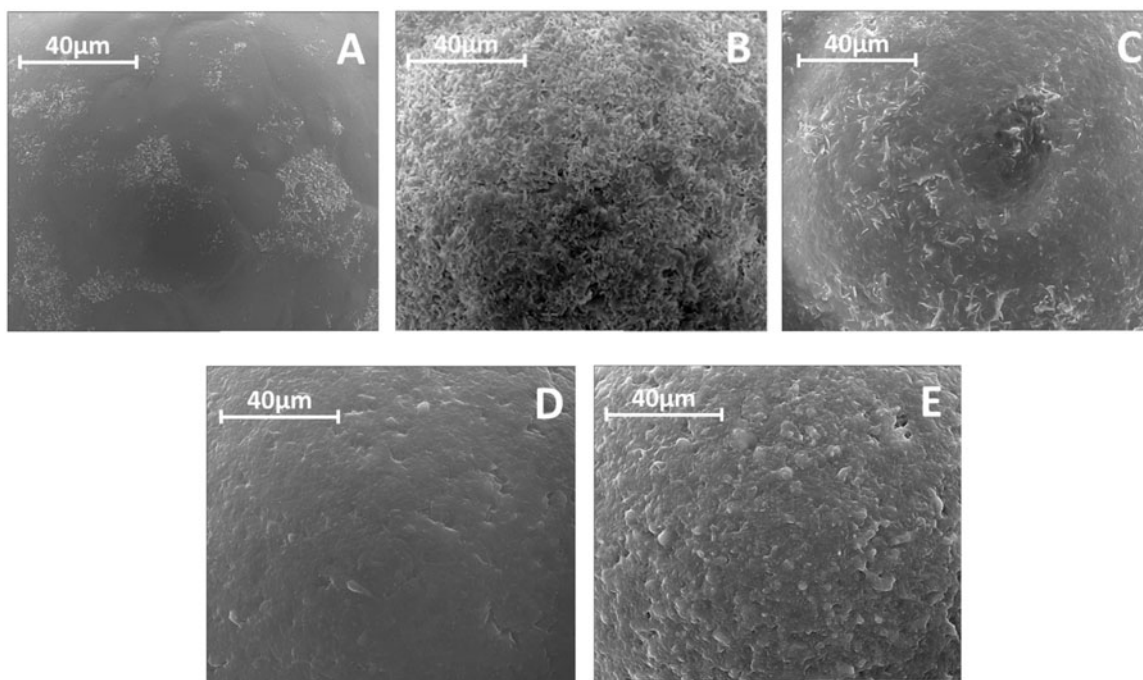
The flowability of the microparticles was determined by the angle of repose method. Microparticles with an essential oil concentration of up to  $150 \text{ gkg}^{-1}$  had excellent flow properties and angle of repose values between  $24.7^\circ$  and  $28.7^\circ$ . At an essential oil concentration of  $225 \text{ gkg}^{-1}$ , the flowability of the microparticles was passable (angle of repose  $45.9^\circ$ ) or at  $300 \text{ gkg}^{-1}$ , poor (angle of repose  $50.8^\circ$ ). It seems that microparticles with such high essential oil concentrations have more surface essential oil than the less loaded microparticles, therefore have a greasy surface and tend to stick together. In this case, they do not behave as single particles but as agglomerates. The worsened flow behaviour of the microparticles with 225 or  $300 \text{ gkg}^{-1}$  essential oil again shows that accurate material dosing might be difficult especially when the microparticles are only added in a small amount.

### 3.5. Appearance and surface structure

Under the light microscope, the microparticles with  $0 \text{ gkg}^{-1}$  essential oil appeared spherical and

**Table 2.** Melting peak maxima and melting enthalpies of unprocessed hydrogenated fat flakes and essential oil containing microparticles.

Essential oil [gkg <sup>-1</sup> ]	Melting range ( $T_m$ ) [°C]	$T_{m_{max1}}$ [°C]	$T_{m_{max2}}$ [°C]	$\Delta H_{m1}$ [J/g]	$\Delta H_{m2}$ [J/g]
Unprocessed hydrogenated fat flakes	34–82	59	71	95 (63 %)	53 (37 %)
0	35–79	57	69	116 (85 %)	21 (15 %)
75	36–82		71		176
150	29–80		68		176
225	30–76		66		154
300	27–73		62		143

**Figure 2.** Light microscopy of microparticles with 0 gkg<sup>-1</sup> (A) and with 75 gkg<sup>-1</sup> (B) essential oil showing the difference between transparent and opaque appearances.**Figure 3.** Scanning electron microscopy pictures of microparticles with different essential oil concentrations: 0 (A), 75 (B), 150 (C), 225 (D) and 300 gkg<sup>-1</sup> (E) showing extensive fat blooming (B) and different, round-shaped structures (D and E).

transparent (Figure 2(A)). With essential oil, the microparticles kept their sphericity; however, their surface became more opaque. This effect was mostly pronounced for the microparticles with the lowest essential oil concentration. Those particles had a clear netlike surface structure (Figure 2(B)). All the other microparticles with essential oil are not shown.

As it was not possible to determine the reason for the differently appearing surface structures as function of the essential oil concentration from the light microscopic pictures alone, the microparticles were also investigated via scanning electron microscopy (Figure 3).

The surface of microparticles with 0 gkg<sup>-1</sup> essential oil was smooth and comprised some agglomerates of

minor developed flake-like structures. Microparticles with  $75 \text{ gkg}^{-1}$  essential oil were almost completely covered with erect, micron-sized flake-like structures. With increasing essential oil concentration the number of those structures decreased and they tended to nestle to the microparticles. The surface of microparticles with  $225 \text{ gkg}^{-1}$  essential oil was mainly smooth with some small, round-shaped structures, the number and height of which increased when the essential oil concentration was  $300 \text{ gkg}^{-1}$ . The flake-like structures appearing on the surfaces of microparticles with 0 and with  $75 \text{ gkg}^{-1}$  essential oil are known as fat blooming and widely studied, especially in the chocolate industry (Yasuda *et al.* 1979, Loisel *et al.* 1997, Mayama 2009, Lopes *et al.* 2015). Fat blooming can either be caused by polymorphic transformation of triglycerides, meaning that the transformation from a less stable crystalline state to a more stable state occurs (Bricknell and Hartel 1998). Other than that fat blooming can be driven by fat migration through a semi-solid matrix and the recrystallization of the fat at the surface of the investigated material. Migration fat blooming is in general promoted by the presence of liquid compounds in a material mixture (De Graef *et al.* 2005) or by increased storage or process temperatures, known as tempering (Ali *et al.* 2001, Lopes *et al.* 2015). In case of the microparticles studied in this work, the fat-blooming effect is obviously promoted in the presence of  $75 \text{ gkg}^{-1}$  essential oil and reduced with essential oil concentrations of  $150 \text{ gkg}^{-1}$  and higher. Based on the scanning electron microscopy pictures, it is not clear whether crystallization is suppressed or if the liquid content of the microparticles is just too high to enable the formed crystals to unbend. As an example, the microparticles with  $150 \text{ gkg}^{-1}$  essential oil exhibited fat crystals. Compared to the crystalline structure of the

microparticles with less essential oil, the crystals were larger and nestled to the surface of the microparticles. A similar study was performed by Yang and Ciftci (2016) who produced peppermint oil loaded hollow nano- and microparticles via carbon dioxide atomisation. The occurrence and the strength of fat-blooming on the surface of the particles varied with the essential oil concentration. As the authors did not investigate particles without essential oil, they discussed the occurrence of fat blooming as a result of the increased essential oil evaporation observed for the microparticles with lower initial essential oil concentration (5 and 10% v/v). However, the current study showed that fat blooming is also observed for microparticles without essential oil and at least in this case cannot be a result of essential oil evaporation.

To investigate whether the morphological differences were a result of changes in the crystallinity of the microparticles, differential scanning calorimetry and X-ray diffraction powder scattering were performed.

### 3.6. Melting behaviour

The differential scanning calorimetric (DSC) signals of the unprocessed hydrogenated fat flakes and the microparticles with  $0 \text{ gkg}^{-1}$  essential oil were compared to investigate the influence of the process on the melting behaviour of the fat. Both signals exhibited two transitions and a shoulder in the same temperature ranges. The sum of the melting enthalpies of the two products were similar, however, the peak area distribution differed. While the microparticles preferably melted at lower temperature, the energy uptake of the unprocessed hydrogenated fat flakes was similar at both temperatures (Figure 4(A)). Following the work of Schoenitz *et al.* (2014), the two distinct transitions in the melting curves of the unprocessed

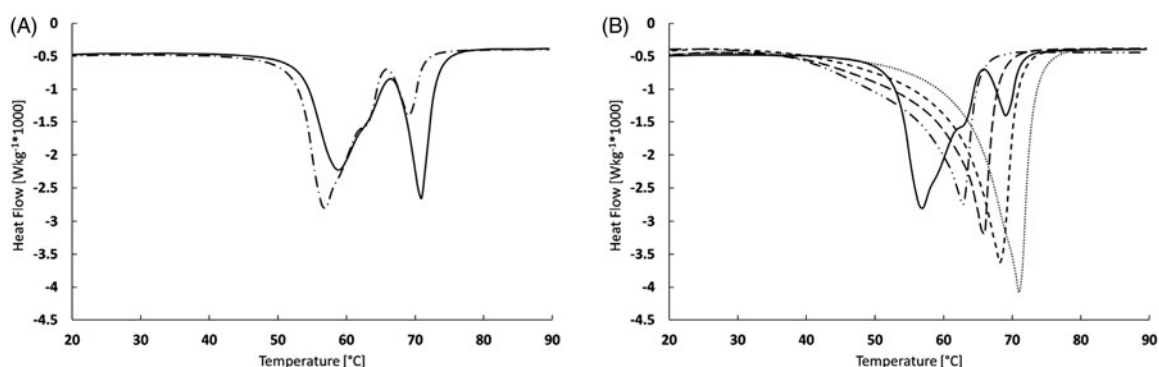


**Figure 4.** (A) Melting curves of the unprocessed fat flakes [—] and the microparticles with  $0 \text{ gkg}^{-1}$  essential oil [---]. (B) Melting curves of microparticles with different concentrations of essential oil: 0 [—], 75 [.....], 150 [----], 225 [— ·] and  $300 \text{ gkg}^{-1}$  [— ·]. The two transitions exhibited by microparticles without essential oil are replaced by a single, broad transition which is dependent on essential oil concentration.

hydrogenated fat flakes and the microparticles with  $0\text{ gkg}^{-1}$  essential oil could be an indication for the presence of different polymorphic forms of a triglyceride. The researchers associated a melting peak at  $42^\circ\text{C}$  to the  $\alpha$ -form of tripalmitin solid lipid nanoparticles and the development of a second melting peak at  $55^\circ\text{C}$  during storage to the transformation of the triglyceride into its  $\beta'$ -form. In consideration of the study of Schoenitz *et al.*, the melting enthalpy shift caused by the spray-chilling process supports the theory of the presence of different polymorphic forms of the triglycerides. The spray-chilling process, characterised by fast material cooling, seems to change the polymorphic composition of the triglycerides in the direction of the polymorphic form with the lower melting point, the  $\alpha$ -form.

In the presence of essential oil, the melting curves of the microparticles exhibited one broad peak, with melting ranges of more than  $50^\circ\text{C}$  (Figure 4(B)). With increasing essential oil concentration, the temperature of the transition maximum decreased from  $71^\circ\text{C}$  with  $75\text{ gkg}^{-1}$  to  $63^\circ\text{C}$  with  $300\text{ gkg}^{-1}$  essential oil. While the microparticles with  $0\text{ gkg}^{-1}$  essential oil started to melt at  $50^\circ\text{C}$  only, melting of the microparticles containing essential oil started already at  $27^\circ\text{C}$  with  $300\text{ gkg}^{-1}$  essential oil and at  $36^\circ\text{C}$  with  $75\text{ gkg}^{-1}$ . The flat slope of the curves at the respective onset temperatures indicates, however, that melting was very little at that stage. All microparticle batches with essential oil, independent from the concentration, had their melting peak maximum at higher temperature compared to the microparticles with  $0\text{ gkg}^{-1}$  essential oil and bigger total melting enthalpies indicating a more stable polymorphic form of the triglycerides. It is known that triglycerides tend to transform into their more stable  $\beta$  and  $\beta'$  crystalline forms under certain conditions, for example throughout storage at

elevated temperature, but also by the addition of limonene (Miyasaki *et al.* 2016). In our case, the essential oil mixture of thymol, carvone, carvacrol and linalool had the same effect. The immediate transition into one of the more stable crystalline forms makes the application of the microparticles in feed mixtures suitable as no changes in their physical properties, such as their melting behaviour or the release of the active ingredients, has to be expected over time.

The exact values from Figure 4 are summarised in Table 2. It shows the melting peak maxima ( $T_{m_{\max}}$ ) and the melting enthalpies ( $\Delta H_m$ ) of the unprocessed hydrogenated fat flakes and the different microparticles.

### 3.7. Crystallinity

X-ray diffraction powder scattering analysis was performed to investigate the crystalline structure of the microparticles and to clarify if the melting peak shifts between the unprocessed hydrogenated fat flakes and the spray-chilled particles consisting of pure hydrogenated fat are driven by polymorphic transformation. Another aim was to clarify if the characteristic melting profile of the microparticles containing essential oil and especially the reduction of the melting peak temperature with increasing essential oil concentration can be explained by polymorphic transformation. Furthermore, the wide angle X-ray scattering signal can be used to determine the crystallinity of a product. A widely applied approach is the construction of the background (Challa *et al.* 1962), indicating that a sustained, convex WAXS range is characteristic for an amorphous material. Regularly arranged peaks in the WAXS signal are a characteristic of the material having a crystalline structure. Figure 5(A) shows the small angle X-ray scattering (SAXS) signals gained for the

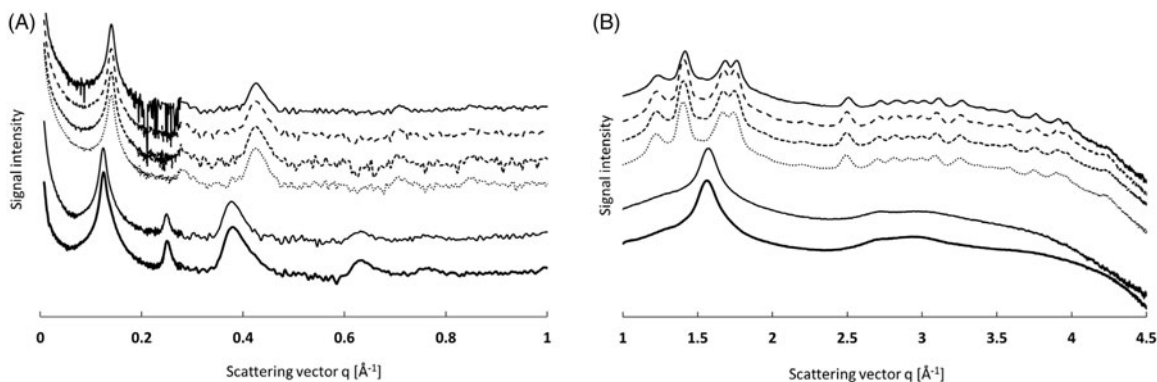


**Figure 5.** (A) SAXS signal and (B) WAXS signal of the unprocessed hydrogenated fat flakes (—), and microparticles with 0 (—), with 75 (·····), 150 (----), 225 (- -) and  $300\text{ gkg}^{-1}$  (—) essential oil. Plots were shifted along the y-axis to avoid overlapping of the peaks. The signals indicate a  $\alpha$ -polymorphic structure without essential oil and a transition to the  $\beta$ -form independent of the essential oil concentration.

unprocessed hydrogenated fat flakes and the microparticles without and with different concentrations of essential oil. The spray-chilling process itself did not have any influence on the crystalline structure of the hydrogenated fat. Both the unprocessed hydrogenated fat flakes and the microparticles without essential oil had a first scattering vector ( $q_{01}$ ) at  $0.124 \text{ \AA}^{-1}$ , a second vector ( $q_{02}$ ) at  $0.25 \text{ \AA}^{-1}$  and a third vector ( $q_{03}$ ) at  $0.36 \text{ \AA}^{-1}$ , corresponding to the (001), (002) and (003) spectrum of a double chain-length structure (Takeuchi *et al.* 2002). With the addition of essential oil  $q_{01}$  shifted to  $0.14 \text{ \AA}^{-1}$ ,  $q_{02}$  to  $0.28 \text{ \AA}^{-1}$  and  $q_{03}$  to  $0.42 \text{ \AA}^{-1}$ . The regular arrangement of several scattering vectors can be associated with the classic lamellar structure of triglycerides. Knowing  $q_{01}$  the thickness ( $d$ ) of a lamellar structure can be calculated with  $d = 2\pi/q_{01}$  (Lopes *et al.* 2015). For the products without essential oil, this yields in a lamellar thickness of  $50.65 \text{ \AA}$  which corresponds to the  $\alpha$ -polymorphic form of tristearin. The microparticles with essential oil exhibit a lamellar thickness of  $44.86 \text{ \AA}$ , representing the  $\beta$ -form of the tristearin polymorphs (Lavigne *et al.* 1993). Varying the essential oil concentration did not influence the lamellar structure.

Figure 5(B) shows the wide angle X-ray scattering (WAXS) signal of the unprocessed hydrogenated fat flakes and the microparticles with different essential oil concentrations. The profiles of the unprocessed hydrogenated fat flakes and of the microparticles with  $0 \text{ gkg}^{-1}$  essential oil were identical. Together with one single peak at  $1.57 \text{ \AA}^{-1}$ , corresponding to a hexagonal arrangement of the short range order of the  $\alpha$ -polymorphic form of tristearin, these curves exhibited a sustained, convex WAXS range without any further peaks. The WAXS signal of the microparticles containing essential oil showed numerous regularly arranged peaks in the range above  $2 \text{ \AA}^{-1}$ , featuring structures with plane distances smaller than  $3.1 \text{ \AA}$ , which were arranged on a sustained, convex shoulder as well.

The small angle and the wide angle X-ray scattering signal indicate that processing itself did not influence the crystalline structure of the hydrogenated fat. Additionally, the wide angle X-ray scattering signal, with its sustained convex shoulder, revealed that both the unprocessed hydrogenated fat flakes and the microparticles without essential oil have an amorphous character. The SAXS and the WAXS signal of the microparticles containing essential oil differed from the signals of the microparticles without essential oil. The first peak in the SAXS signal, characterising the lamellar structure of a crystalline structure, was shifted. This shift was identical for all essential oil concentrations.

The WAXS signal with a row of regularly ordered peaks indicates the crystallinity of the microparticles containing essential oil. Since the crystalline structure of the microparticles containing essential oil did not change as a function of the essential oil concentration, just a small amount of the essential oil seems to be responsible for the crystalline structure. Combining the results from the DSC analysis and from the X-ray diffraction powder scattering it can be concluded that the essential oil supports the formation of certain crystalline structures.

#### 4. Conclusion

The particle size distribution, the essential oil recovery, the flowability, the surface structure, the melting behaviour and the crystalline structure of microparticles with 0, 75, 150, 225 and  $300 \text{ gkg}^{-1}$  essential oil were investigated. After production all produced microparticle batches were free-flowing with essential oil recoveries around 90%. The essential oil concentration had a strong effect on the flowability, the surface structure and the melting profile of the microparticles. Also, processing alone had an obvious effect on the melting behaviour of the hydrogenated fat. The crystallinity of the applied triglycerides was not affected by the spray-chilling process alone but only by the presence of essential oil. However, crystallinity was not dependent on the essential oil concentration of the microparticles.

#### Disclosure statement

No potential conflict of interest was reported by the author(s).

#### Funding

This study was supported by the BIOMIN Holding GmbH. The authors want to thank BIOMIN for their financial and scientific support.

#### ORCID

Stephen Cole  <http://orcid.org/0000-0001-9618-4606>

#### References

- Ali, A., *et al.*, 2001. Effect of storage temperature on texture, polymorphic structure, bloom formation and sensory attributes of filled dark chocolate. *Food chemistry*, 72 (4), 491–497.

- Alvim, I.D., *et al.*, 2013. Use of spray chilling method to deliver hydrophobic components: physical characterization of microparticles. *Ciência e tecnologia de alimentos*, 33, 34–39.
- Bakry, A.M., *et al.*, 2016. Microencapsulation of oils: a comprehensive review of benefits, techniques and applications. *Comprehensive reviews in food science and food safety*, 15(1), 143–182.
- Bento, M.H.L., *et al.*, 2013. Essential oils and their use in animal feeds for monogastric animals - Effects on feed quality, gut microbiota, growth performance and food safety: a review. *Veterinarni medicina*, 58, 449–458.
- Bricknell, J. and Hartel, R.W., 1998. Relation of fat bloom in chocolate to polymorphic transition of cocoa butter. *Journal of the American Oil Chemists' Society*, 75 (11), 1609–1615.
- Challa, G., Hermans, P.H., and Weidinger, E., 1962. On the determination of the crystalline fraction in isotactic polystyrene from X-ray diffraction. *Die makromolekulare chemie*, 56, 169–178.
- De Graef, V., *et al.*, 2005. Prediction of migration fat bloom on chocolate. *European journal of lipid science and technology*, 107 (5), 297–306.
- El Asbahani, A., *et al.*, 2015. Essential oils: from extraction to encapsulation. *International journal of pharmaceuticals*, 483 (1–2), 220–243.
- Gately, S. F., Wright, D. R., and Valagene, R. J., 2009. Granular feed supplement. United States Patent 2009/0092704.
- Gibbs, B.F., *et al.*, 1999. Encapsulation in the food industry: a review. *International journal of food sciences and nutrition*, 50 (3), 213–224.
- Himawan, C., Starov, V.M. and Stapley, A.G.F., 2006. Thermodynamic and kinetic aspects of fat crystallization. *Advances in colloid and interface science*, 122 (1–3), 3–33.
- Jackson, L.S., and Lee, K., 1991. Microencapsulation and the food industry. *Lebensmittel wissenschaft und technologie*, 24, 289–297.
- Klose, R. E. 2000. Encapsulated bioactive substances. United States Patent 6,013,286.
- Lavigne, F., Bourgaux, C., and Ollivon, M., 1993. Phase transitions of saturated triglycerides. *Le journal de physique IV*, 3, 137–140.
- Loisel, C., *et al.*, 1997. Fat bloom and chocolate structure studied by mercury porosimetry. *Journal of food science*, 62 (4), 781–788.
- Lopes, D.G., *et al.*, 2015. Role of lipid blooming and crystallite size in the performance of highly soluble drug-loaded microcapsules. *Journal of pharmaceutical sciences*, 104 (12), 4257–4265.
- Lumay, G., *et al.*, 2012. Measuring the flowing properties of powders and grains. *Powder technology*, 224, 19–27.
- Madene, A., *et al.*, 2006. Flavour encapsulation and controlled release - a review. *International journal of food science and technology*, 41 (1), 1–21.
- Mayama, H., 2009. Blooming theory of tristearin. *Soft matter*, 5 (4), 856–859.
- Miyasaki, E.K., *et al.*, 2016. Acceleration of polymorphic transition of cocoa butter and cocoa butter equivalent by addition of D-limonene. *European journal of lipid science and technology*, 118 (5), 716–723.
- Murugesan, G.R., *et al.*, 2015. Phytochemical feed additives as an alternative to antibiotic growth promoters in broiler chickens. *Frontiers in veterinary science*, 2 (21). doi: [10.3389/fvets.2015.00021](https://doi.org/10.3389/fvets.2015.00021)
- Popplewell, L. M. and Porzio, M. A., 2001. Fat-coated encapsulation compositions and method for preparing the same. United States Patent 6,245,366.
- Sato, K., 2001. Crystallization behaviour of fats and lipids - a review. *Chemical engineering science*, 56 (7), 2255–2265.
- Schoenitz, M., *et al.*, 2014. Controlled polymorphic transformation of continuously crystallized solid lipid nanoparticles in a microstructured device: a feasibility study. *European journal of pharmaceuticals and biopharmaceuticals*, 86 (3), 324–331.
- Singh, M.N., *et al.*, 2010. Microencapsulation: a promising technique for controlled drug delivery. *Research in pharmaceutical sciences*, 5 (2), 65–77.
- Suresh, G., *et al.*, 2018. Alternatives to antibiotics in poultry feed: molecular perspectives. *Critical reviews in microbiology*, 44 (3), 318–335.
- Takeuchi, M., Ueno, S., and Sato, K., 2002. Crystallization kinetics of polymorphic forms of a molecular compound constructed by SOS (1,3-distearoyl-2-oleoyl-*sn*-glycerol) and SSO (1,2-distearoyl-3-oleoyl-*rac*-glycerol). *Food research international*, 35 (10), 919–926.
- Vishwakarma, G.S., *et al.*, 2016. Polymeric encapsulates of essential oils and their constituents: a review of preparation techniques, characterization and sustainable release mechanisms. *Polymer reviews*, 56 (4), 668–701.
- Yang, J. and Ciftci, O.N., 2016. Development of free-flowing peppermint essential oil-loaded hollow solid lipid micro- and nanoparticles via atomization with carbon dioxide. *Food research international*, 87, 83–91.
- Yasuda, N., *et al.*, 1979. Cocoa butter substitutes and their preparation. United States Patent 4,157,405.
- Zeng, Z., *et al.*, 2015. Essential oil and aromatic plants as feed additives in non-ruminant nutrition: a review. *Journal of animal science and biotechnology*, 6 (1), 7.